

Selection of Peptide–Bismuth Bicycles Using Phage Display

Ruo-Nan He, Meng-Jie Zhang, Bin Dai,* and Xu-Dong Kong*

Cite This: <https://doi.org/10.1021/acschembio.4c00099>

Read Online

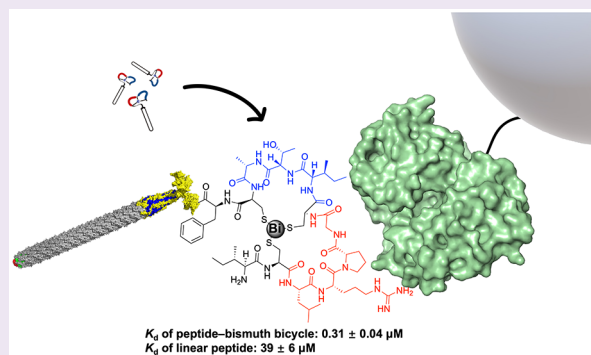
ACCESS |

Metrics & More

Article Recommendations

Supporting Information

ABSTRACT: Cysteine conjugation is widely used to constrain phage displayed peptides for the selection of cyclic peptides against specific targets. In this study, the nontoxic Bi^{3+} ion was used as a cysteine conjugation reagent to cross-link peptide libraries without compromising phage infectivity. We constructed a randomized 3-cysteine peptide library and cyclized it with Bi^{3+} , followed by a selection against the maltose-binding protein as a model target. Next-generation sequencing of selection samples revealed the enrichment of peptides containing clear consensus sequences. Chemically synthesized linear and Bi^{3+} cyclized peptides were used for affinity validation. The cyclized peptide showed a hundred-fold better affinity ($0.31 \pm 0.04 \mu\text{M}$) than the linear form ($39 \pm 6 \mu\text{M}$). Overall, our study proved the feasibility of developing Bi^{3+} constrained bicyclic peptides against a specific target using phage display, which would potentially accelerate the development of new peptide–bismuth bicycles for therapeutic or diagnostic applications.



Cyclic peptides stand out in drug development for their superior affinities and selectivities to the broad, flat surfaces of protein targets.^{1,2} They can be rapidly synthesized by solid-phase peptide synthesis, which enables the incorporation of labels affording diverse chemical and biological attributes,³ such as enhanced tissue permeability^{4–6} and broader administration routes.^{7,8} Moreover, the rigidity of cyclic peptides reduces their conformational flexibility, which in turn enhances their therapeutic efficacy.^{3,4,8,9}

Due to the compatibility with various chemical modifications^{7,10,11} and the feasibility of large peptide library construction,¹² phage display is a versatile and widely applied method for the identification of cyclic peptides against a given target. Peptide libraries could be customized to be compatible with different cyclization strategies. Conversely, the cyclization conditions should be optimized so as not to lose the infectivity of the phage. One of the widely used approaches involves the formation of a disulfide bond between two cysteine residues,¹³ which has no toxicity on phage infectivity but suffers from redox sensitivity. The alkylating linkers are also popularly used to modify the side chains or N-terminus of peptides for the phage selection of monocyclic, bicyclic and double-bridged peptides.⁷

More recently, the metal ion Bi^{3+} (bismuth) was reported as a stable, rigid, nontoxic and selective linker in bicyclization of peptides by reacting with the cysteine residues.^{14–16} Motivated by the insights from in situ access to constrained peptides with Bi^{3+} ,¹⁵ our research focused on developing Bi^{3+} as a cysteine conjugation reagent to generate the phage displayed bicyclic peptide library (Figure 1). We report the phage selection of

peptide–bismuth bicycles against maltose binding protein (MBP), which yielded cyclic peptides with hundred-fold better affinity than the linear form. These results not only confirm the viability of Bi^{3+} as a linker in phage selection but also highlight its potential to significantly enhance peptide affinity to target proteins, providing valuable insights for peptide engineering in therapeutic applications.

As part of the selection procedure, phage displayed 3-cysteine peptides were cyclized with Bi^{3+} and then selected against a model target. Cysteines in the phage displayed peptides were designed to be reduced with TCEP to restore the free thiol side chains before cyclization using Bi^{3+} . While bismuth is demonstrated as a nontoxic metal even when ingested in large quantities orally (150 mg/kg/day),¹⁷ it may still cause the loss of phage infectivity when combined with TCEP due to the disruption of disulfide bonds in the capsid protein PIII. Therefore, we determined the concentration of bismuth that does not compromise phage infectivity in screening conditions and assessed its efficacy in peptide cyclization. The toxic effect of 0–200 μM of Bi^{3+} on phage infectivity was first characterized. After the reduction with 1 mM of TCEP at 25 °C for 30 min, 200 and 400 μM of Bi^{3+} may cause 1000 to 10000-fold of decrease in phage infectivity,

Received: February 9, 2024

Revised: April 10, 2024

Accepted: April 11, 2024

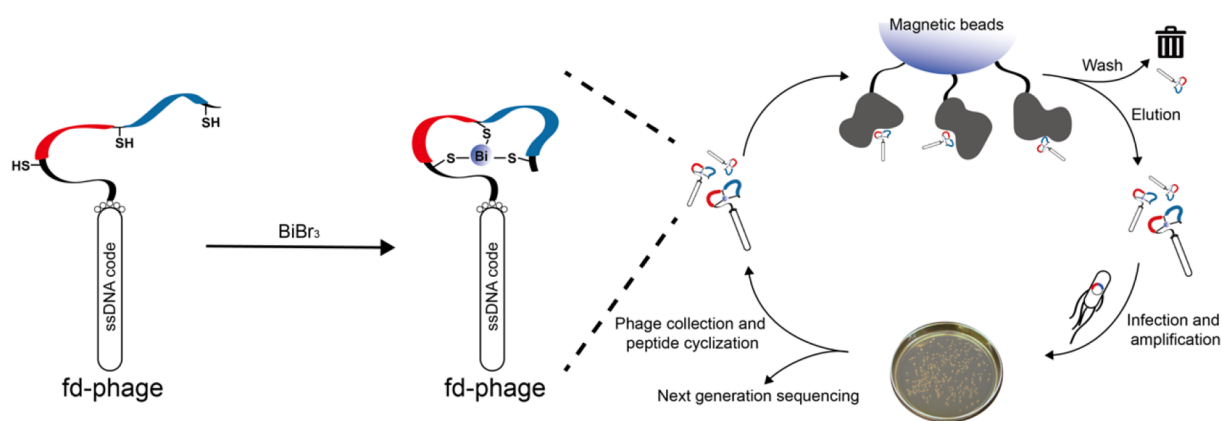


Figure 1. General workflow for the phage selection of peptide–bismuth bicycles. Three-cysteine peptides displayed on the phage were cyclized by Bi^{3+} to generate a diverse bicyclic peptide library. This library underwent affinity selection against immobilized target protein, with nonbinding phages being washed away. Binding phages were eluted, amplified in *Escherichia coli* TG1 cells, and re-entered into successive selection rounds. This iterative process was conducted 3 times to enrich the binders with high affinities. After selection, peptide encoding sequences were amplified from phage samples and analyzed through next-generation sequencing.

while no significant loss of infectivity was observed for Bi^{3+} concentrations below $100 \mu\text{M}$ (Figure 2A).

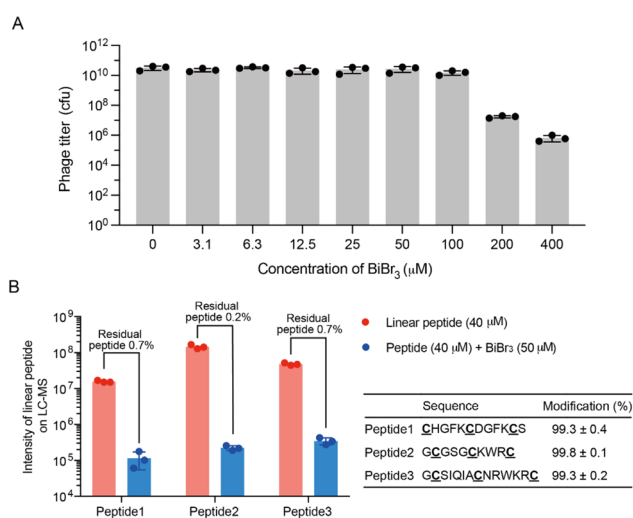


Figure 2. Optimization of conditions for cyclization of phage displayed peptides using Bi^{3+} . A) The toxic effect of BiBr_3 on phage infectivity. After sequential treatment with 1 mM TCEP and 0–400 μM of BiBr_3 , phage titers were determined ($n = 3$). Data in the figure are shown as the mean \pm SD. B) Cyclization efficacy of BiBr_3 (at $50 \mu\text{M}$) on 3-cysteine linear peptides determined by LC-MS. Intensity of the linear form peptides on LC-MS were measured ($n = 3$) before and after cyclization to quantify the extent of cyclization. Data in the table are shown as the mean \pm SD.

To evaluate the efficacy of bismuth cyclization at nontoxic concentrations for phage infectivity, a series of experiments were conducted by incubating linear peptides with BiBr_3 , followed by quantifying the cyclized peptide with LC-MS. According to the research of Nitsche et al., Bi^{3+} at the millimolar concentration can efficiently cyclize 3-cysteine linear peptides to generate peptide–bismuth bicycles under physiological conditions.¹⁵ Bi^{3+} at this concentration may, however, results in a loss of phage infectivity and interfere with the implementation of phage selection. Therefore, further characterization of the Bi^{3+} cyclization efficiency at lower

concentrations was required. In addition, the study of Nitsche et al. indicated that peptides with 3–5 residues between cysteines presented higher yield of cyclization. Accordingly, peptides 1–3 were synthesized with format of $\text{CX}_4\text{CX}_4\text{C}$, $\text{CX}_3\text{CX}_3\text{C}$ and $\text{CX}_5\text{CX}_5\text{C}$ as shown in Figure 2B. The analysis of Bi^{3+} cyclized peptides on HPLC showed difficulties in the separation of linear and cyclized peptides, and a significant difference of UV absorbance for the two forms of peptide (Figure S1). As a result, the cyclization extent of peptides in the presence of $50 \mu\text{M}$ Bi^{3+} was quantitatively determined using LC-MS. By determining the amounts of linear peptides before and after cyclization, the percentage of peptides (at $40 \mu\text{M}$) cyclized with $50 \mu\text{M}$ of Bi^{3+} reached 99.3–99.8% for peptides 1–3 (Figure 2B). Considering that the molar concentration of phage displayed peptides during the selection usually falls in the range of 10 pM to 10 nM, it is evident that $50 \mu\text{M}$ Bi^{3+} is sufficient for cyclizing phage displayed peptide library for further selection.

Subsequently, we designed and constructed a phage library named the RN-library, displaying 3-cysteine peptides suitable for Bi^{3+} cyclization. The peptides were designed with the format of $\text{XCX}_m\text{CX}_n\text{CX}$ ($m, n = 3, 4, \text{ or } 5$) containing a random amino acid at both ends and three cysteines spaced by different numbers of random amino acids, yielding 9 different backbone formats (Figure 3A). The plasmids containing sequences encoding peptide library were constructed through the self-ligation of whole-plasmid PCR products¹² and then introduced into *E. coli* TG1 cells by electroporation. This procedure facilitated the generation of a peptide library with approximately 1×10^9 members, limited by the efficiency of transformation.

To assess the quality of the RN-library, the peptide encoding sequences inserted into the phage plasmid were amplified and characterized with next generation sequencing (NGS). Out of 172,052 reads from NGS, 56% of sequences coded for peptides that containing exactly three cysteines (Figure 3B), while 9% containing two cysteines possibly caused by the errors introduced in the synthesis of DNA primers. The remaining 35% of sequences contained additional cysteines derived from the random amino acid positions coded by the NNK codon. Subsequently, the peptide sequences were grouped into the sublibraries according to their backbone formats (cysteine

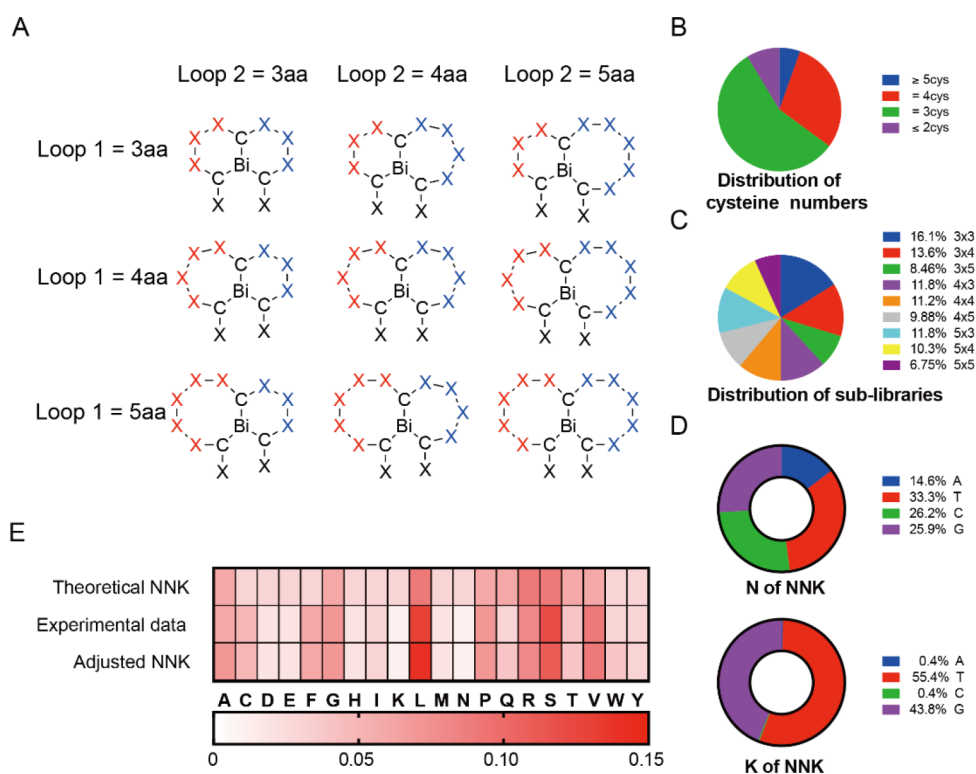


Figure 3. Peptide formats and the quality of the phage library. A) Patterns of bicycled peptides displayed on phage. The peptides have lengths between 11 and 15 amino acids consisting of 3 cysteines (C) and 8 to 12 random amino acids (X). The library was cloned using 10 degenerate DNA primers (Table S2) in which the random amino acids were encoded by NNK codons. The red and blue colors show the two randomized loop segments. B) Distribution of peptides containing different numbers of cysteines in the peptide library. C) Proportion of the 9 sublibraries. D) Frequency of nucleotides coding the random amino acids. E) Theoretical, adjusted NNK coding peptides and experimental frequency of all amino acids at the random positions of the peptide library.

positions). As shown in Figure 3C, the proportion of each sublibrary ranges from 6.75 to 16.1% with relatively equal distribution. The DNA and amino acid sequences at random positions were extracted and analyzed. As shown in Figure 3D, A, T, C, and G nucleotides at the “N” positions have frequencies of 14.6%, 33.3%, 26.2%, and 25.9%, respectively. For the position “K” of the NNK codon, frequencies of 55.4% and 43.9% are observed for nucleotides T and G, while frequencies of A and C are both 0.4%. Overall, the nucleotide distribution at the “N” and “K” positions of the NNK codon shows a significant deviation from what was expected, which most likely resulted from the insufficient quality of primers used in the construction of the RN-library.

Next, we analyzed the distribution of 20 amino acids at the random positions of the peptide library. Sublibraries of 3 × 3 and 5 × 5 were taken as examples (Figure S2) to demonstrate that the distribution of amino acids at different random positions of the peptides is consistent. Turning into details, the experimental data from our library have a clear bias compared with the theoretical distribution of NNK codon (Figure 3E), which could be calculated from the proportion of 1/32 to 3/32 for amino acids with 1 to 3 codons. In contrast, the experimental data were consistent with the distribution of amino acid calculated from the adjusted NNK codon, which was based on the experimental frequencies of nucleotides. In addition, based on the adjusted NNK codon, cysteine has a probability of 4.87% to appear at the random position. We calculated the probability to have cysteine at the random positions for each sublibrary (Table S1), which would

theoretically lead to the overall of 39.2% peptides with more than 3 cysteines, in good agreement with our experimental data of 38.4% (ignoring the 2-cys fraction, Figure 3B). In summary, we can conclude that the inconsistency between the experimentally determined amino acid distribution and the theoretical distribution of NNK codon is resulted from the bias in the nucleotide ratio discussed above and not by biological bias due to phage amplification.

For the selection of target-specific peptide–bismuth bicycles, MBP was served as a model target. The RN-library was cultured overnight to amplify the phage displaying cysteine rich peptides. Cysteines of peptides were then reduced with TCEP, followed by cyclization with Bi³⁺ at 50 μM in a pH 8.0 reaction buffer. As a control, an additional copy of the phage sample was treated similarly but without Bi³⁺. The two samples were panned separately against biotinylated MBP that immobilized on magnetic streptavidin (round1 and round3) or neutravidin (round2) beads. For the first round of selection, 6.0 × 10¹² phages were purified from 250 mL of culture and 5.0 × 10⁵ to 1.7 × 10⁶ of them were captured by the target after panning (Figure S3). The captured phages were used to infect the *E. coli* TG1 cells and plated on 14 cm diameter agar plates. Conventional phage selection protocols typically involve collecting cells from the plate for inoculation in fresh liquid culture, amplifying the phage for a subsequent round of selection. As a simplified protocol, in this study, we collected the phage directly from the agar plates of each round affording phage titer >4.0 × 10¹¹, which was sufficient to cover the diversity of enriched peptides of each round. After three

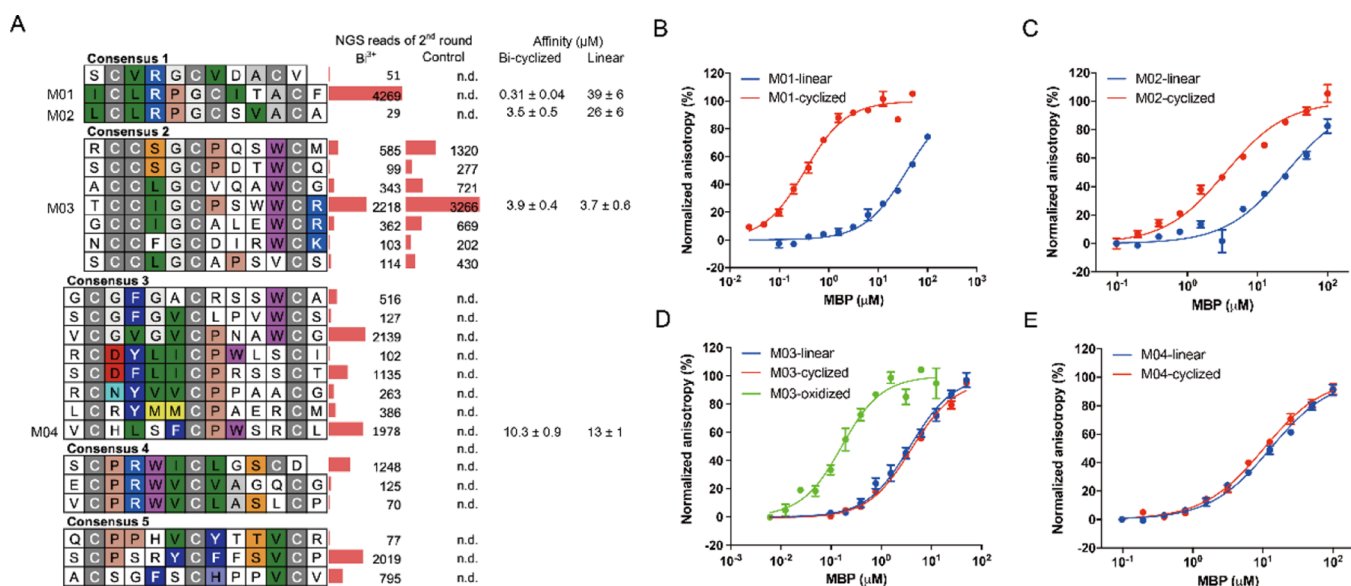


Figure 4. Phage selections performed against MBP. A) Alignment of peptides in groups based on sequence similarities. The abundance of the sequences enriched in the 2nd round of selection is indicated. The red frames represent the relative abundance of each sequence in the NGS results. B–E) The binding affinity (K_D) of peptides, labeled at the C-terminus with fluorescein, was determined by fluorescence polarization. Data are shown as the mean of 3 biologically independent measurements.

rounds of selection, the capture yields (eluted phage/loaded phage) of panning increased from 7.8×10^{-7} to 2.6×10^{-5} for the Bi³⁺ cyclized selection and from 2.9×10^{-6} to 1.3×10^{-4} for the control selection, indicating the successful enrichment of target binding peptides (Figure S3).

Subsequently, the DNA sequence of the phage samples in each round were amplified by PCR using primers equipped with unique barcode sequences and sequenced by Illumina novaseq platform. MatLab scripts were used to separate the sequences of different samples according to the barcodes, translate the nucleotide sequences into amino acid sequences and classify the peptide sequences into different consensus groups.¹⁸ As shown in Figure 4A, five consensus groups could be identified from the NGS data of the second round. Consensus 1 and consensus 3–5 peptides containing 3 cysteines showed specificity in Bi³⁺ cyclization selection over the control selection. In contrast, consensus 2 peptides containing 4 cysteines existed in both the Bi³⁺ cyclization and control selection with very similar relative abundance. An analysis of the total abundance of 3-cysteine and 4-cysteine peptides in Bi³⁺ cyclization and control selection showed a significant difference (Figure S4). Since a 4-cysteine peptide may form a double-bridged peptide through the formation of two disulfide bonds, the specific enrichment of 4-cysteine peptides in the control selection was most likely due to the reoxidation of cysteines in the cyclization and panning steps. In addition, the NGS data of round 3 showed a huge increase in the proportion of consensus 2 peptides both in the control and the Bi³⁺ cyclization selection (Figure S5). The reason for this was speculated to be the insufficient reduction of peptides displayed on the phage during library preparation, affecting the cyclization of peptides with Bi³⁺ and increased the presence of double-bridged peptides.

Finally, to validate the binding affinity of enriched sequences, four peptides from the consensus groups were synthesized with a C-terminal fluorescein moiety, cyclized with Bi³⁺, and tested by fluorescence polarization for affinity characterization (Figure 4B–E). The peptide M01 from

consensus 1 showed submicromolar affinity ($K_D = 0.31 \pm 0.04 \mu\text{M}$) after cyclization, while the binding of its linear counterpart is more than a hundred folds weaker ($K_D = 39 \pm 6 \mu\text{M}$, Figure 4B). Similarly, another peptide from consensus 1 (M02) also gained better affinity ($K_D = 3.5 \pm 0.5 \mu\text{M}$) after cyclization, yet the K_D of the linear form of M02 against MBP is $26 \pm 6 \mu\text{M}$. The linear form of the other two peptides M03 and M04 in consensus 2 and 3 displayed weak affinities for MBP in the micromolar range, which was not improved by cyclization with Bi³⁺. As expected, the oxidized M03 peptide with a double-bridged scaffold exhibited higher affinity ($K_D = 0.14 \pm 0.03 \mu\text{M}$, Figure 4D), confirmed that the consensus 2 peptides were enriched as the oxidized form instead of the Bi³⁺ cyclized form during the selection. Regardless, the results of consensus 1 peptides verified that Bi³⁺ modification may generate bicyclic peptides with new structures capable of binding to the target protein. This expansion in structural diversity would potentially increase the likelihood of identifying target-specific peptides with high affinity through phage selection.

In summary, we introduced the nontoxic Bi³⁺ as a new linker to generate the phage displayed bicyclic peptide library without compromising the phage infectivity, thereby expanding the repertoire of tools available for library diversification. To assess the impact of Bi³⁺ cross-linking, a library displayed peptides in the format of XCX_mCX_nCX (m, n = 3, 4, or 5) was constructed and selected against MBP as the target protein. The results demonstrated the identification of peptides with remarkable improvement in affinity when cyclized with Bi³⁺. Notably, one bicyclic peptide M01 exhibited a hundredfold stronger affinity for MBP compared to its linear counterpart. This finding underscores the potential of Bi³⁺ as a valuable linker in the construction of the macrocycle libraries.

Bicyclic peptides have gained increasing attention due to their superior stabilities and high affinities against target proteins. Nitsche et al. have recently demonstrated the possibility and therapeutic potential of bismuth-peptide bicycles that penetrate human cell membranes effectively.⁶

Meanwhile, phage display is a widely used approach for identifying bicyclic peptides with specific binding properties. Our study validated the feasibility of using phage display to select novel bismuth-peptide bicycles for a given target, which may accelerate the discovery of more peptide scaffolds that can be efficiently constrained with Bi³⁺, as well as new cyclic peptides for therapeutic or diagnostic applications.

■ ASSOCIATED CONTENT

SI Supporting Information

The Supporting Information is available free of charge at <https://pubs.acs.org/doi/10.1021/acscchembio.4c00099>.

Supplementary results about the construction of phage displayed peptide library, next generation sequencing of the peptide library and additional experimental details, materials, and methods; Supplementary tables with the details of library construction; Supplementary figures with results of peptide LC-MS characterization, phage selection and NGS results (PDF)

■ AUTHOR INFORMATION

Corresponding Authors

Bin Dai – School of Sensing Science and Engineering, School of Electronic Information and Electrical Engineering, Shanghai Jiao Tong University, Shanghai 200240, China; orcid.org/0000-0002-2386-4413; Email: daibin@sjtu.edu.cn

Xu-Dong Kong – State Key Laboratory of Microbial Metabolism and School of Life Sciences and Biotechnology, Shanghai Jiao Tong University, Shanghai 200240, China; Zhangjiang Institute for Advanced Study, Shanghai Jiao Tong University, Shanghai 201203, China; orcid.org/0000-0003-3216-7545; Email: xudong.kong@sjtu.edu.cn

Authors

Ruo-Nan He – School of Sensing Science and Engineering, School of Electronic Information and Electrical Engineering and State Key Laboratory of Microbial Metabolism and School of Life Sciences and Biotechnology, Shanghai Jiao Tong University, Shanghai 200240, China; Zhangjiang Institute for Advanced Study, Shanghai Jiao Tong University, Shanghai 201203, China

Meng-Jie Zhang – State Key Laboratory of Microbial Metabolism and School of Life Sciences and Biotechnology, Shanghai Jiao Tong University, Shanghai 200240, China; Zhangjiang Institute for Advanced Study, Shanghai Jiao Tong University, Shanghai 201203, China

Complete contact information is available at: <https://pubs.acs.org/doi/10.1021/acscchembio.4c00099>

Notes

The authors declare no competing financial interest.

■ ACKNOWLEDGMENTS

This work was financially supported by the National Natural Science Foundation of China (22107066).

■ REFERENCES

- (1) Arkin, M. R.; Wells, J. A. Small-Molecule Inhibitors of Protein–Protein Interactions: Progressing towards the Dream. *Nat. Rev. Drug Discovery* **2004**, *3* (4), 301–317.
- (2) Zorzi, A.; Deyle, K.; Heinis, C. Cyclic Peptide Therapeutics: Past, Present and Future. *Curr. Opin. Chem. Biol.* **2017**, *38*, 24–29.
- (3) Malde, A. K.; Hill, T. A.; Iyer, A.; Fairlie, D. P. Crystal Structures of Protein-Bound Cyclic Peptides. *Chem. Rev.* **2019**, *119* (17), 9861–9914.
- (4) Dougherty, P. G.; Sahni, A.; Pei, D. Understanding Cell Penetration of Cyclic Peptides. *Chem. Rev.* **2019**, *119* (17), 10241–10287.
- (5) Peraro, L.; Kritzer, J. A. Emerging Methods and Design Principles for Cell-Penetrant Peptides. *Angew. Chem., Int. Ed.* **2018**, *57* (37), 11868–11881.
- (6) Voss, S.; Adair, L. D.; Achazi, K.; Kim, H.; Bergemann, S.; Bartschlagler, R.; New, E. J.; Rademann, J.; Nitsche, C. Cell-Penetrating Peptide-Bismuth Bicycles. *Angew. Chem., Int. Ed.* **2024**, *63*, e202318615.
- (7) Kong, X.-D.; Moriya, J.; Carle, V.; Pojer, F.; Abriata, L. A.; Deyle, K.; Heinis, C. De Novo Development of Proteolytically Resistant Therapeutic Peptides for Oral Administration. *Nat. Biomed. Eng.* **2020**, *4* (5), 560–571.
- (8) Nielsen, D. S.; Shepherd, N. E.; Xu, W.; Lucke, A. J.; Stoermer, M. J.; Fairlie, D. P. Orally Absorbed Cyclic Peptides. *Chem. Rev.* **2017**, *117* (12), 8094–8128.
- (9) Hill, T. A.; Shepherd, N. E.; Diness, F.; Fairlie, D. P. Constraining Cyclic Peptides To Mimic Protein Structure Motifs. *Angew. Chem., Int. Ed.* **2014**, *53* (48), 13020–13041.
- (10) Ekanayake, A. I.; Sobze, L.; Kelich, P.; Youk, J.; Bennett, N. J.; Mukherjee, R.; Bhardwaj, A.; Wuest, F.; Vukovic, L.; Derda, R. Genetically Encoded Fragment-Based Discovery from Phage-Displayed Macrocyclic Libraries with Genetically Encoded Unnatural Pharmacophores. *J. Am. Chem. Soc.* **2021**, *143* (14), 5497–5507.
- (11) Chen, S.; Lovell, S.; Lee, S.; Fellner, M.; Mace, P. D.; Bogyo, M. Identification of Highly Selective Covalent Inhibitors by Phage Display. *Nat. Biotechnol.* **2021**, *39* (4), 490–498.
- (12) Kong, X.-D.; Carle, V.; Díaz-Perlas, C.; Butler, K.; Heinis, C. Generation of a Large Peptide Phage Display Library by Self-Ligation of Whole-Plasmid PCR Product. *ACS Chem. Biol.* **2020**, *15* (11), 2907–2915.
- (13) Hansen, S.; Zhang, Y.; Hwang, S.; Nabhan, A.; Li, W.; Fuhrmann, J.; Kschonsak, Y.; Zhou, L.; Nile, A. H.; Gao, X.; Piskol, R.; de Sousa e Melo, F.; de Sauvage, F. J.; Hannoush, R. N. Directed Evolution Identifies High-Affinity Cystine-Knot Peptide Agonists and Antagonists of Wnt/ β -Catenin Signaling. *Proc. Natl. Acad. Sci. U. S. A.* **2022**, *119* (46), No. e2207327119.
- (14) Mohan, R. Green Bismuth. *Nat. Chem.* **2010**, *2* (4), 336–336.
- (15) Voss, S.; Rademann, J.; Nitsche, C. Peptide–Bismuth Bicycles: In Situ Access to Stable Constrained Peptides with Superior Bioactivity. *Angew. Chem., Int. Ed.* **2022**, *61*, No. e20211385.
- (16) Cordero, B.; Gómez, V.; Platero-Prats, A. E.; Revés, M.; Echeverría, J.; Cremades, E.; Barragán, F.; Alvarez, S. Covalent Radii Revisited. *Dalton Trans.* **2008**, *21*, 2832–2838.
- (17) Figueroa-Quintanilla, D.; Salazar-Lindo, E.; Sack, R. B.; Leon-Barua, R.; Sarabia-Arce, S.; Campos-Sanchez, M.; Eyzaguirre-Maccan, E. A Controlled Trial of Bismuth Subsalicylate in Infants with Acute Watery Diarrheal Disease. *N. Engl. J. Med.* **1993**, *328* (23), 1653–1658.
- (18) Rentero Rebollo, I.; Sabisz, M.; Baeriswyl, V.; Heinis, C. Identification of Target-Binding Peptide Motifs by High-Throughput Sequencing of Phage-Selected Peptides. *Nucleic Acids Res.* **2014**, *42* (22), No. e169.